

A NOVEL LASER SHOCK SURFACE PATTERNING PROCESS TOWARD TRIBOLOGICAL APPLICATIONS

Bo Mao, Arpith Siddaiah, Pradeep L. Menezes, Yiliang Liao*

Department of Mechanical Engineering, University of Nevada, Reno, Reno, NV 89557 USA

Corresponding author email: yliao@unr.edu

ABSTRACT

We report a novel laser-based surface processing process, laser shock surface patterning (LSSP) integrating both surface strengthening and patterning effects might lead to broader impacts in tribology research and applications. This process utilizes the laser-induced shockwave loadings to introduce the surface strengthening and patterning effects simultaneously, leading to the fabrication of arrays of micro-indentations or protrusions for the enhanced wear resistance and manipulated friction values. Two process designs, direct-LSSP and indirect-LSSP were proposed and carried out on AZ31B Mg alloys and AISI 1045 steels, respectively. The 3D surface profiles of the samples after LSSP were characterized. The hardness of surface patterns prepared by laser processing was measured. The friction values as affected by laser processing parameters were measured by sliding tests. The relationships among laser processing parameters, micro-feature characteristics, and COF were discussed.

Keywords: Laser Shock Processing; Coefficient of Friction; Surface Strengthening; Surface Patterning.

INTRODUCTION

Friction and wear are two major concerns in various engineering applications where surface interactions exist [1]. Extensive research efforts have been paid in tribology research which emphasizes on improving the wear resistance and manipulating the friction value. The wear resistance determines the durability and reliability of engineering components. In the metal forming process, like extrusion, rolling, the friction force between the ingot and forming tools plays an important role on the process performance and final product properties [2].

A variety of surface modification methods, such as plasma electrolytic oxidation [3], thermal oxidation [4], anodizing [5], and laser cladding [6], have been developed to improve their

tribological performance. For instance, Rapheal et al. [3] reduced the coefficient of friction (COF) of MRI 230D Mg alloy by 50% using plasma electrolytic oxidation to fabricate a surface layer of hard crystalline ceramic. Fabre et al. [6] produced a Al-Si coating on ZE41 Mg alloy by laser cladding, and found that the COF was increased by 67% and the wear resistance was 2.5 times higher than that of the as-cast sample. However, most of these methods focus on developing a hard surface coating and are typically cost- and time- consuming. Moreover, unsatisfied bonding strength at interface and some environmental issues are associated with these processes.

Surface texturing or patterning has been proved to be another effective surface modification approach for improving the tribological properties of metallic materials [7-14]. The texture features can be utilized to control the contacting areas, trap wear debris and lubricants during sliding, and therefore manipulate the COF and improve the wear resistance of processed materials [15, 16]. For instance, Walker et al. [17] applied electrochemical machining to a hypereutectic Al-Si alloy surface to generate dimple-decorated texture. It was found that the COF was reduced by up to 38.5% and the wear debris was effectively removed during sliding. Yuan et al. [18] fabricated micro-grooves on the surface of boron-copper alloy cast iron using photolithography. It was found that the COF can be tuned by adjusting the angle between the grooves and sliding direction. Hu et al. [19] reported that the COF and wear of Ti-6Al-4V under lubrication condition were both reduced by producing dimple texture on the surfaces using laser surface texturing (LST). Among various surface texturing approaches, LST has gained much more interests due to its high flexibility, good controllability, and superior texturing accuracy. It has been applied to many engineering fields including bearings, sliding seals, and gears [20-24]. However, the surface patterns generated by LST are mostly through laser ablation, which might introduce the undesirable tensile residual stresses and surface softening effect on the processed surface [25].

In this paper, a novel laser-based surface processing process, named laser shock surface patterning (LSSP) is

developed. Two process designs named direct-LSSP and indirect-LSSP were proposed. This approach utilizes laser shock processing instead of laser ablation to introduce surface hardening and surface texturing effect, both of which contribute to improving tribological properties. The direct-LSSP experiments were performed on an AZ31B Mg alloy and indirect-LSSP experiments were performed on AISI 1045 steels to fabricate surface textures of micro-indentations with various depths. The surface morphology and the microstructure evolution of the samples during LSSP process were characterized. The surface hardening effect induced by LSSP process was analyzed. The tribological performance of the processed samples were evaluated.

EXPERIMENTAL PROCEDURE

Materials

LSSP experiments were carried out on AISI 1045 carbon steel square plates and AZ31B Mg alloys blocks with 1 inch width and 0.5 inch thickness. Prior to LSSP, the samples were ground using SiC sand paper (up to 1200 grit), followed by fine polishing with 1 μ m diamond suspension to obtain a random surface texture with a roughness of ~ 20 nm.

LSSP process

The schematic configurations of the sample assembly and LSSP process are illustrated in Figure 1. During the direct-LSSP process (Figure 1(a)), a reflective coating was put on the surface of the sample. A mold with micro-features is applied to the top surface of the reflective coating. A transparent confinement is applied as the uppermost component of the sample assembly. When the high-energy laser pulse is directed onto the target surface, this micro-feature materials will be instantaneously vaporized and ionized, leading to the formation of plasma with high temperature and high pressure [26]. The expansion of the plasma is confined by the transparent confinement and resulting the high shockwave pressure, which propels the mold into the substrate material to generate protruded micro-features. The configuration of indirect-LSSP process is illustrated in Figure 1b. In the indirect-LSSP process, a micro-mold with micro-features is placed on the target surface. The absorptive coating material is evenly sprayed or coated on top of the micro-mold to absorb the laser energy and protect micro-molds and target surfaces from undesired laser damages. On top of the absorptive coating, a transparent confinement is placed to constrain the hydrodynamic expansion of laser-induced plasma for the generation of laser-induced shockwave with a high peak pressure. Once the peak pressure of laser-induced shockwave is higher than the dynamic yield strength of the target material, the high strain rate surface plastic deformation is induced, leading to the fabrication of anti-skew surfaces with arrays of micro-indentations [27]. In this process, the micro-mold serves as a mask and a cushion for patterning, and does not directly interact with laser energy. As compared with LST by

direct laser ablation, during LSSP process, the laser energy does not directly interact with the substrate material, thus avoiding heating-induced tensile residual stress and softening effect.

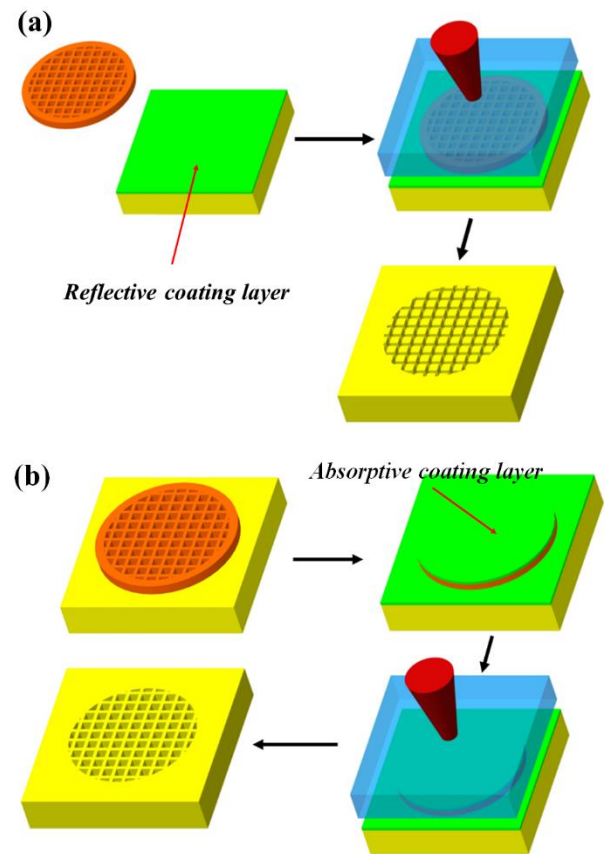


Figure 1: A schematic illustration of LSSP process: (a) direct-LSSP and (b) indirect-LSSP.

In this study, a Surelite III Q-switched Nd:YAG laser (Continuum Inc.) with a wavelength of 1064 nm and a pulse duration of 5 ns was used to deliver the laser energy. The laser beam diameter was adjusted to 3 mm, and each surface pattern was obtained by LSSP with five pulses to reduce the error introduced by the beam energy variance. A copper grid (G400, Ted Pella Inc.) with a diameter of 3.05 mm was used as the mold. The BK7 glass was used as the confining medium. Graphite and aluminum foil were used as absorptive layer and reflective layer materials respectively. Finally, the patterned substrate was ultrasonically cleaned with ethanol after peeling off the coating and mold.

Characterization and Mechanical Property Testing

The surface morphology of the Mg alloy and steels samples processed by LSSP was characterized by a scanning electron microscope (SEM, JEOL-2100) and a 3D optical profilometer (Rtec Instruments). Hardness measurements were conducted on unprocessed and patterned surfaces using a Wilson

hardness tester operated with a 100g load (for Mg alloy sample) and 300 g (for steel sample) and a 10s holding time. The tribological tests were performed with an Rtec Multi-function tribometer 5000 using a ball-on-plate sliding configuration in ambient environment. Samples before and after LSSP processing were fixed on the lower stage, while AA3003 aluminum alloy ball (McMaster-Carr) with a diameter of 6.35 mm was mounted as the upper sample. The sliding condition for steel samples are 50 N in load and 2 mm/s in sliding velocity. While they are 5 N for Mg alloy and 0.1 mm/s for Mg alloy samples. The variation of COF with sliding distance was recorded in each test.

RESULTS AND DISCUSSION

Surface micro-patterns prepared by LSSP

Figure 2 shows an optical image of the copper grid used as the mold during the LSSP process. It has a bar width of 12 μm , hole width of 50 μm , and pitch width of 62 μm . Figure 2(b) shows a SEM image of patterned surface produced by LSSP with a laser intensity of 1.47 GW/cm^2 . It is evident that the micro-feature from the mold have been successfully transferred to the surface of Mg alloy sample substrate. Figure 2(c) and 2(d) are the 3D optical image and one-dimensional profile of the surface pattern, respectively. It can be observed that the micro-grooves have a width of $\sim 10 \mu\text{m}$ and the square bumps have a width of $\sim 50 \mu\text{m}$, which have similar dimensions to the bars and holes of the grid, respectively. The average depth of micro-grooves is measured to be $2.02 \pm 0.17 \mu\text{m}$ in this case, and it is expected to be adjusted by changing the laser intensity. During the LSSP experiment in our study, the copper grid was punched into the Mg alloy sample substrate by laser-induced shockwave pressure. The substrate surface areas underneath the bars of the grid thus experienced plastic deformation, while the areas underneath the holes of the grid were not directly subject to this shock loading. As a result, the surface with protruded micro-features was generated, i.e., the micro-grooves was formed and the square bumps were left on the surface.

Figure 3 shows the surface morphology of the specimen generated by LSSP with a laser intensity of 0.554 GW/cm^2 . As observed in Figure 3, the shape of the mold (TEM copper grid) is well taken by the substrate, showing array of squared indentations with a width of 37 μm . The observed micro-indentations indicate that a severe plastic deformation is induced by laser shock loadings in the hole areas of TEM grid. On the other hand, in the bar areas of TEM grid, no significant deformation is observed as the mechanical energy of laser shockwave is absorbed by the copper grid, which serves as a cushion layer. Figure 3(b) and 3(c) show a 3-D image and a 1-D profile of micro-indentations, respectively. It is observed that the indentation depth generated by LSSP is around $0.43 \pm 0.07 \mu\text{m}$.

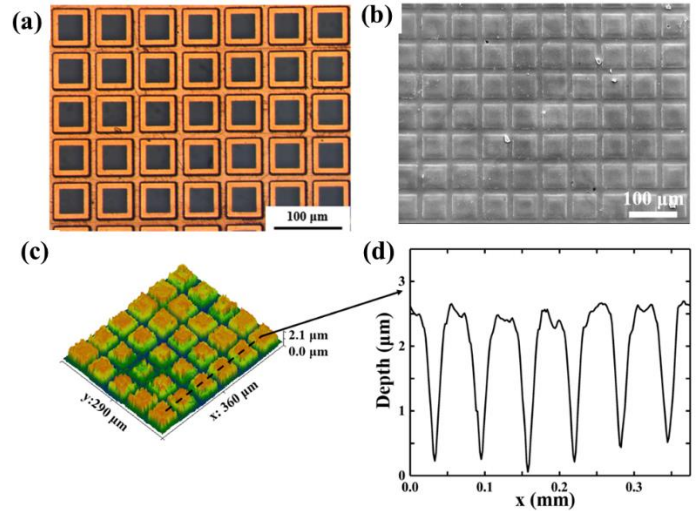


Figure 2: (a) An optical image of the copper grid used in this study, (b) a SEM image of the patterned surface of Mg alloy sample processed by direct-LSSP with a laser intensity of 1.47 GW/cm^2 , (c) a 3D image of the patterned surface of Mg alloy sample, (d) a 1D profile of the micro-grooves and square bumps of Mg alloy sample.

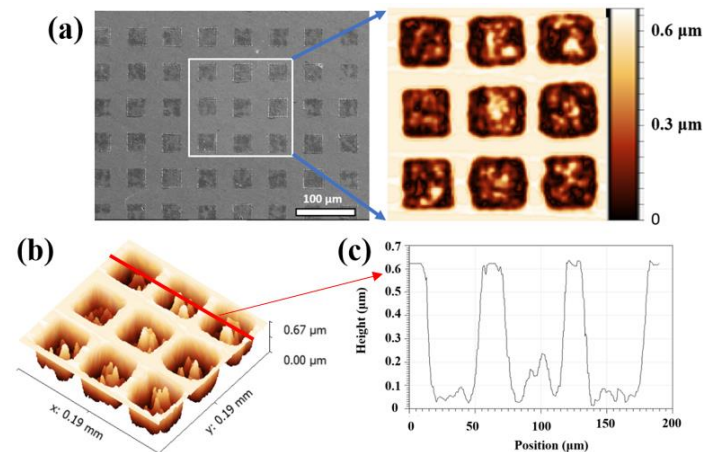


Figure 3: (a) A SEM image and a 2-D optical image of the patterned surface of steel sample processed by in-direct LSSP with a laser intensity of 0.554 GW/cm^2 , (b) a 3-D image of patterned micro-indentations, and (c) a 1-D profile of micro-indentations.

Surface hardening induced by LSSP

Figure 4 presents the micro-hardness of patterned surfaces produced by LSSP with different laser intensities. For the Mg alloy samples processed by direct-LSSP, it is found that for LSSP with a laser intensity less than 1.92 GW/cm^2 , the micro-hardness of patterned surface increases with the increase of laser intensity. For instance, the surface hardness increases from 81 to 72.9 HV as the laser intensity increases from 1.47 to 1.12 GW/cm^2 . At

a laser intensity of 1.92 GW/cm^2 , the surface hardness reaches a maximum value of 88 HV. Further increasing laser intensity led to the surface hardening saturation phenomenon and has been observed in previous studies [28, 29]. For Mg alloys, surface hardening effect induced by LSSP is attributed to the twinning microstructure, which has been reported in the literature via two major mechanisms: (1) Hall-Petch effect caused by twinning-induced grain refinement [30], and (2) texture hardening induced by crystal lattice reorienting like deformation twinning from a softer orientation to a harder orientation [31]. For the steel samples processed by indirect-LSSP. It can be seen that the hardness value increases by increasing the laser power intensity (Figure 4(b)). For instance, the hardness increases from 212 VHN (Vickers Hardness Number) for the untreated specimen to 238 VHN for the specimen processed by LSSP with a laser intensity of 0.890 GW/cm^2 . The hardness improvement is attributed to the work hardening effect induced by laser shock loading, and is expected to lead to enhanced wear resistance of the LSSP treated specimen.

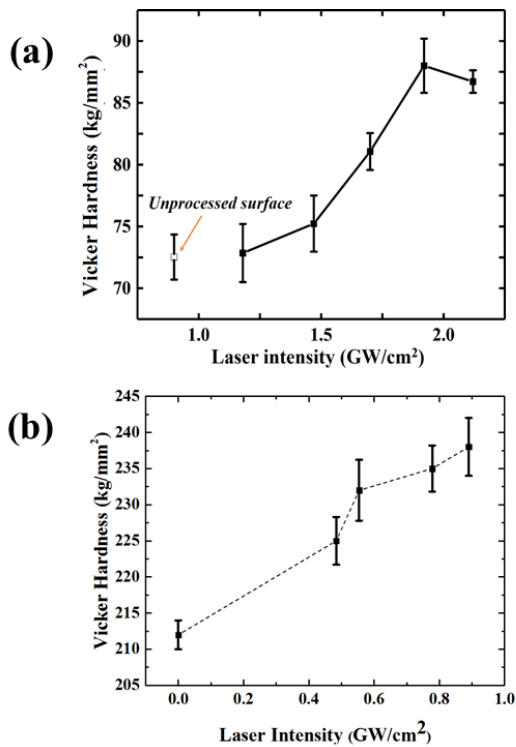


Figure 4: Variation of surface hardness of samples with laser intensity: (a) AZ31B Mg alloy sample processed by direct-LSSP and (b) AISI4140 steel sample processed by indirect-LSSP.

Tribological properties as affected by LSSP

Cross-over scratch tests were carried out to study the patterning effect introduced by LSSP on the friction value. Particular focus is put on the transition from unprocessed area

(marked as smooth surface) to the processed area (marked as patterned surface). For the Mg alloy samples processed by direct-LSSP, it is found that the average COF is 0.151 for the smooth surface, and reduced to 0.124 for the patterned surface (Figure 5(a)). For the steel samples processed by indirect-LSSP, it is observed that the COF is dramatically reduced from 0.36 to 0.28 from the base surface to the laser-patterned surface (Figure 5(b)). This reduction of COF by surface patterning was also reported in a few other work [32, 33], which is typically explained by the reduction of real are of contact. For example, Rosenkranz et al. [32] fabricated various textures on 42CrMo4 steel using laser ablation. It was found that the COF is reduced from 0.118 to 0.108 for line-like pattern with a periodicity of 15 μm . Byun et al. [34] produced micro-dimples on the surface of AISI 440C steel with electrochemical machining, and reported a significant reduction of COF at low-speed condition. Li et al. [35] showed that the hot-embossed patterned micro-features on a bulk metallic glass could reduce its COF from 1.05 to 0.45. Bathe et al. [36] reported that a dramatic drop of COF on the surface of a gray cast iron was achieved by laser surface texturing. They both attributed the reduction of COF to the decrease of contact area during the sliding due to the existence of skew micro-patterns. Further, Menezes et al. [37] reported that the COF can be manipulated over 200% by patterning the surfaces.

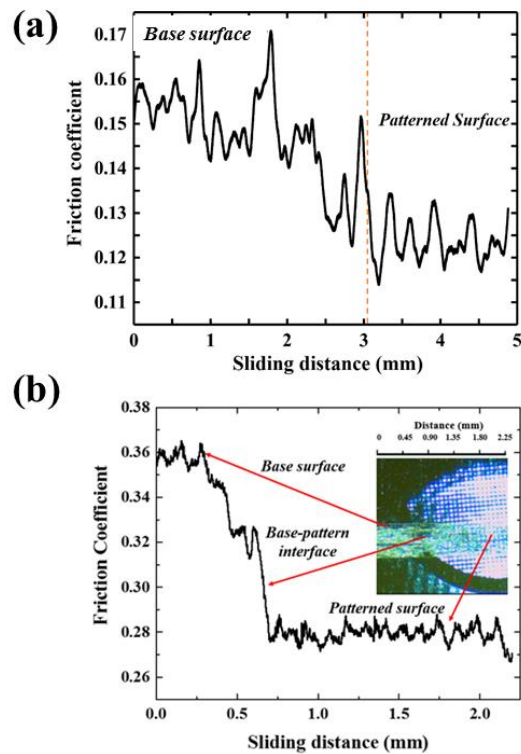


Figure 5: Cross-over scratch tests under a dry condition. (a) The COF of Mg alloy samples on base and patterned surfaces prepared by direct-LSSP with a laser intensity of 1.70 GW/cm^2

and (b) the COF of steel sample processed by indirect-LSSP with a laser intensity of 0.554 GW/cm².

The COF of patterned surface of the Mg alloy samples processed by direct-LSSP as affected by laser intensity was measured and depicted in Figure 6. It is observed that the COF of all patterned surfaces are lower than that of the smooth surface (unprocessed). However, the COF decreases first, and then reaches a saturation value with increasing laser intensity. For example, COF decreases to 0.143, 0.134 and 0.124 at laser intensity of 1.18, 1.47 and 1.70 GW/cm², respectively. Further increasing the laser intensity shows negative effects on the reduction of COF. It is observed that the COF reduces to a minimum value of 0.118 at laser intensity of 1.92 GW/cm², and slightly increases to 0.125 when laser intensity reaches 2.12 GW/cm².

The value of COF is generally determined by friction force F_f resulting from sliding and normal force F_n through: $\mu = F_f / F_n$. The total friction force F_f is consisted of adhesion friction force F_{ad} and friction force responsible for mechanical deformation F_{de} . As reported by Bowden et al. [38], the adhesion component is proportional to the real contact area A_r by: $F_{ad} = A_r \times \tau$, where τ is the interfacial shear strength. The mechanical deformation component F_{de} is strongly related to the degree of plastic deformation. By producing surface pattern on Mg alloys with LSSP, the real contact area is reduced, leading to the decrease of adhesion force. In addition, the laser shock induced surface hardening effect may alleviate the plastic deformation during sliding test [39-41], thus decreasing the deformation force. Therefore, the COF is reduced after LSSP processing as a result of the decreased total friction force.

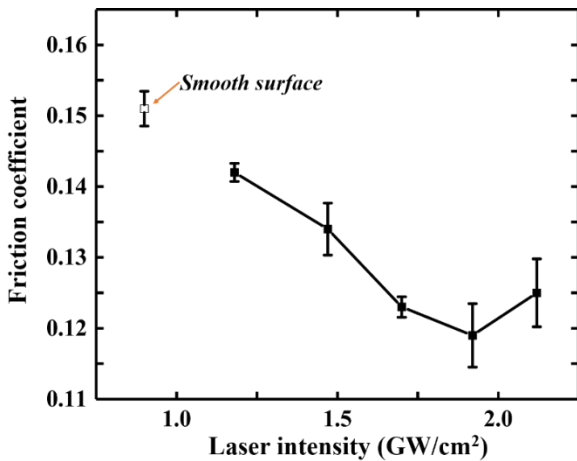


Figure 6: The COF of patterned surface of Mg alloy samples produced by direct-LSSP with various laser intensities.

Indirect-LSSP experiments were conducted with various laser intensities to study the effect of laser intensity on COF of steel samples, as shown in Figure 7. It can be seen that the friction value of laser patterned surface can be manipulated by

adjusting the laser intensity. As an example, given a low laser intensity of 0.484 and 0.554 GW/cm², the COF was reduced by 55% and 26% from 0.38 to 0.17 and 0.28, respectively. On the other hand, given a high laser intensity of 0.778 and 0.890 GW/cm², the COF was increased by 45% and 87% from 0.38 to 0.55 and 0.71, respectively.

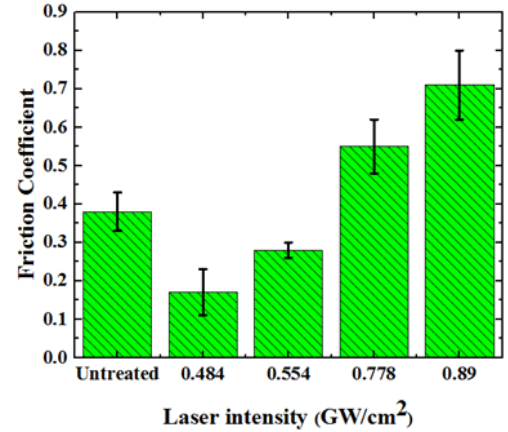


Figure 7: The COF of patterned surface of steel samples produced by indirect-LSSP with various laser intensities.

This relationship between COF and laser intensity results from the combination effect of surface patterning surface hardening effect. For the direct-LSSP process, the surface protrusions were fabricated. At low laser intensities, the plastic deformation only takes place in a very small area. Hence, the surface hardening effect is almost negligible and only patterning effect dominates the reduction of friction coefficient, which can be explained by the decrease of contact area due to the micro-grooves [16]. As laser intensity increases, further reduction of COF is mainly attributed to the increased plastic deformation and surface crystallographic texture change. The increase of groove depth may have a minimal effect on the friction performance since dry scratch test is applied in this study [42]. As the plastic deformation approaches its saturation point at high laser intensities, the surface hardness increases to a maximum value (88 HV at 1.92 GW/cm² in this study), and hence the COF is reduced to a minimum value. Further increasing the laser intensity leads to the twinning saturation, which weakens the efficiency for reducing COF. On the other hand, with the grid being punched into the target, part of the deformed substrate material tends to pile up at the edges of square bumps, generating bulges higher than the initial substrate surface [43]. As shown in Figure 8, these bulges become obvious for patterned surface with high laser intensities, resulting in the surface roughening effect. For example, the surface roughness increased from 167 nm to 456 nm as the laser intensity increased from 1.18 to 2.12 GW/cm². The roughed surface tend to hinder the relative movement between tribo-pairs, thus increasing the friction force. Therefore, a slightly increase of COF at laser intensity higher than 1.92 GW/cm² was identified in Figure 8.

Figure 9 schematically illustrates the laser intensity effect on the contact conditions between the pin and patterned substrate of steel samples prepared by indirect-LSSP. At a high laser intensity as 0.890 GW/cm^2 , due to the deeper indentation depth and the narrower bands, the penetration depth of the sliding pin at the tribo-pair interface is deeper, as compared to it is under the condition sliding against the patterned surface prepared by LSSP with a low laser intensity such as 0.448 GW/cm^2 . This deeper penetration is attributed to more stress concentration induced by the sharper edge geometry, which leads to that a greater shear stress is needed to sustain sliding. Moreover, as the surface roughening effect increases with the increased laser intensity, there might be more asperities interlocking at the indentation bottom areas. These changes of surface morphology lead to the increase of COF with the increased laser intensity. According to experimental results and analysis, it can be seen that for a patterned surface, the determination of the COF is much more complex than an untreated flat surface. It involves mechanisms including the resistance force from the indentation edge, the interlocking of asperities at the tribo-pair interfaces, and the change of surface strength [1]. A quantitative relationship between the COF and the surface patterning parameters needs to be further investigated.

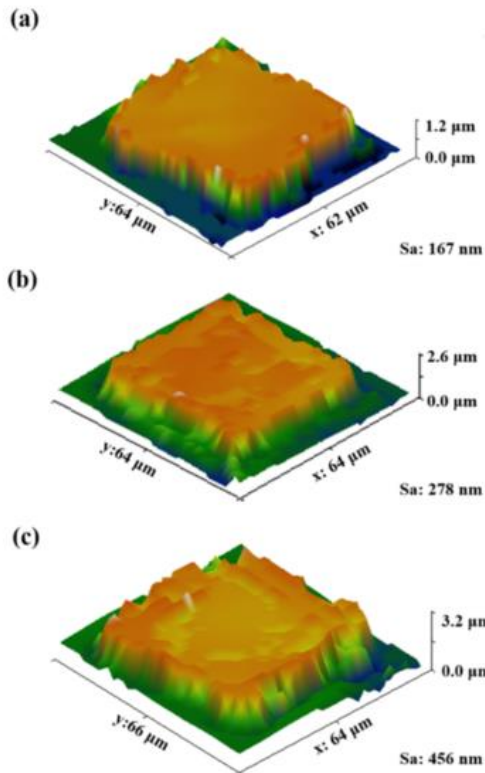


Figure 8: Surface morphologies of square bumps protruded with laser intensity of (a) 1.18, (b) 1.70, and (c) 2.12 GW/cm^2 .

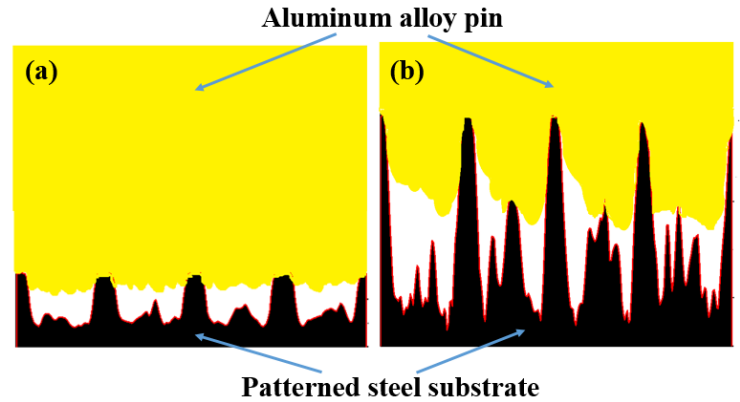


Figure 9: Schematic illustration of contact conditions between the aluminum alloy pin and the patterned steel substrate processed by LSSP with a laser intensity of (a) 0.448 GW/cm^2 and (b) 0.890 GW/cm^2 .

CONCLUSIONS

In this paper, a novel laser-based surface patterning process, named LSSP, is proposed and studied in this paper. This process utilizes the laser-induced shockwave loadings to introduce the surface strengthening and patterning effects simultaneously. Moreover, two process designs, direct-LSSP and indirect-LSSP were realized and carried on AZ31B Mg alloys and AISI 4140 steels, respectively. The direct-LSSP process resulted in surface patterns with protrusions and indirect-LSSP process resulted in surface indentations. Both processes were able to improve the surface hardness of the studied materials. The surface COF as affected by laser intensities in LSSP process was studied. It was found that both direct and indirect-LSSP process brought a lowered COF at low laser intensity as compared with unprocessed surface, while further increasing the laser intensity resulted in elevated COF due to surface roughening effect. We envision that further investigation and development of LSSP process will lead to the fabrication of patterned surfaces with desired tribology properties, in particular the manipulated COF and the enhanced wear resistance. Therefore, LSSP has a great potential in widespread industrial applications.

REFERENCES

- [1] Menezes PL, Ingole, S.P., Nosonovsky, M., Kailas, S.V., Lovell, M.R., Tribology for Scientists and Engineers. New York: Springer-Verlag 2013.
- [2] Taltavull C, Torres B, Lopez A, Rams J. Dry sliding wear behavior of AM60B magnesium alloy. *Wear*. 2013;301:615-25.
- [3] Rapheal G, Kumar S, Blawert C, Dahotre NB. Wear behavior of plasma electrolytic oxidation (PEO) and hybrid coatings of PEO and laser on MRI 230D magnesium alloy. *Wear*. 2011;271:1987-97.

- [4] Majumdar JD, Bhattacharyya U, Biswas A, Manna I. Studies on thermal oxidation of Mg-alloy (AZ91) for improving corrosion and wear resistance. *Surface and Coatings Technology*. 2008;202:3638-42.
- [5] Hino M, Murakami K, Saijo A, Hikino S, Kanadani T. Friction and Wear Properties on AZ91D Magnesium Alloy Treated by Anodizing from Phosphate Electrolytic Solution. *Materials Transactions*. 2011;52:1752-8.
- [6] Fabre A, Masse J-E. Friction behavior of laser cladding magnesium alloy against AISI 52100 steel. *Tribology international*. 2012;46:247-53.
- [7] Garcia-Giron A, Romano J, Liang Y, Dashtbozorg B, Dong H, Penchev P, et al. Combined surface hardening and laser patterning approach for functionalising stainless steel surfaces. *Applied Surface Science*. 2018;439:516-24.
- [8] Joshi B, Tripathi K, Gyawali G, Lee SW. The effect of laser surface texturing on the tribological performance of different Sialon ceramic phases. *Progress in Natural Science: Materials International*. 2016;26:415-21.
- [9] Wakuda M, Yamauchi Y, Kanzaki S, Yasuda Y. Effect of surface texturing on friction reduction between ceramic and steel materials under lubricated sliding contact. *Wear*. 2003;254:356-63.
- [10] Nakano M, Korenaga A, Korenaga A, Miyake K, Murakami T, Ando Y, et al. Applying micro-texture to cast iron surfaces to reduce the friction coefficient under lubricated conditions. *Tribology Letters*. 2007;28:131-7.
- [11] Ryk G, Kligerman Y, Etsion I. Experimental investigation of laser surface texturing for reciprocating automotive components. *Tribology Transactions*. 2002;45:444-9.
- [12] Tang W, Zhou Y, Zhu H, Yang H. The effect of surface texturing on reducing the friction and wear of steel under lubricated sliding contact. *Applied Surface Science*. 2013;273:199-204.
- [13] Pettersson U, Jacobson S. Friction and wear properties of micro textured DLC coated surfaces in boundary lubricated sliding. *Tribology letters*. 2004;17:553-9.
- [14] Mao B, Siddaiah A, Menezes PL, Liao Y. Surface texturing by indirect laser shock surface patterning for manipulated friction coefficient. *Journal of Materials Processing Technology*. 2018;257:227-33.
- [15] Xing Y, Deng J, Wang X, Meng R. Effect of laser surface textures combined with multi-solid lubricant coatings on the tribological properties of Al₂O₃/TiC ceramic. *Wear*. 2015;342-343:1-12.
- [16] Xing Y, Deng J, Feng X, Yu S. Effect of laser surface texturing on Si₃N₄/TiC ceramic sliding against steel under dry friction. *Materials & Design (1980-2015)*. 2013;52:234-45.
- [17] Walker J, Kamps T, Lam J, Mitchell-Smith J, Clare AT. Tribological behaviour of an electrochemical jet machined textured Al-Si automotive cylinder liner material. *Wear*. 2017;376:1611-21.
- [18] Yuan S, Huang W, Wang X. Orientation effects of micro-grooves on sliding surfaces. *Tribology international*. 2011;44:1047-54.
- [19] Hu T, Hu L, Ding Q. The effect of laser surface texturing on the tribological behavior of Ti-6Al-4V. *Proceedings of the Institution of Mechanical Engineers, Part J: Journal of Engineering Tribology*. 2012;226:854-63.
- [20] Wang X, Kato K. Improving the anti-seizure ability of SiC seal in water with RIE texturing. *Tribology letters*. 2003;14:275-80.
- [21] Sinanoğlu C, Nair F, Karamış MB. Effects of shaft surface texture on journal bearing pressure distribution. *Journal of Materials Processing Technology*. 2005;168:344-53.
- [22] Marian VG, Gabriel D, Knoll G, Filippone S. Theoretical and experimental analysis of a laser textured thrust bearing. *Tribology Letters*. 2011;44:335.
- [23] Netzel JP. The effect of interface cooling in controlling surface disturbances in mechanical face seals. *Wear*. 1982;79:119-27.
- [24] Grabon W, Koszela W, Pawlus P, Ochwat S. Improving tribological behaviour of piston ring–cylinder liner frictional pair by liner surface texturing. *Tribology international*. 2013;61:102-8.
- [25] Kusinski J, Kac S, Kopia A, Radziszewska A, Rozmus-Górnikowska M, Major B, et al. Laser modification of the materials surface layer—a review paper. *Bulletin of the Polish Academy of Sciences: Technical Sciences*. 2012;60:711-28.
- [26] Mao B, Liao Y, Li B. Gradient twinning microstructure generated by laser shock peening in an AZ31B magnesium alloy. *Applied Surface Science*. 2018;457:342-51.
- [27] Mao B, Liao Y. Modeling of Lüders elongation and work hardening behaviors of ferrite-pearlite dual phase steels under tension. *Mechanics of Materials*. 2019;129:222-9.
- [28] Siddaiah A, Mao B, Liao Y, Menezes PL. Surface characterization and tribological performance of laser shock peened steel surfaces. *Surface and Coatings Technology*. 2018;351:188-97.
- [29] Montross CS, Wei T, Ye L, Clark G, Mai Y-W. Laser shock processing and its effects on microstructure and properties of metal alloys: a review. *International Journal of Fatigue*. 2002;24:1021-36.
- [30] Hong S-G, Park SH, Lee CS. Role of {10–12} twinning characteristics in the deformation behavior of a polycrystalline magnesium alloy. *Acta Materialia*. 2010;58:5873-85.

- [31] Mao B, Liao Y, Li B. Abnormal twin-twin interaction in an Mg-3Al-1Zn magnesium alloy processed by laser shock peening. *Scripta Materialia*. 2019;165:89-93.
- [32] Rosenkranz A, Krupp F, Reinert L, Mücklich F, Sauer B. Tribological performance of laser-patterned chain links – Influence of pattern geometry and periodicity. *Wear*. 2017;370-371:51-8.
- [33] Zhang C, Yang B, Wang J, Wang H, Liu G, Zhang B, et al. Microstructure and friction behavior of LaF₃ doped Ti-MoS₂ composite thin films deposited by unbalanced magnetron sputtering. *Surface and Coatings Technology*. 2019;359:334-41.
- [34] Byun JW, Shin HS, Kwon MH, Kim BH, Chu CN. Surface texturing by micro ECM for friction reduction. *International Journal of Precision Engineering and Manufacturing*. 2010;11:747-53.
- [35] Li N, Xu E, Liu Z, Wang X, Liu L. Tuning apparent friction coefficient by controlled patterning bulk metallic glasses surfaces. *Scientific Reports*. 2016;6:39388.
- [36] Bathe R, Krishna VS, Nikumb S, Padmanabham G. Laser surface texturing of gray cast iron for improving tribological behavior. *Applied Physics A*. 2014;117:117-23.
- [37] Menezes PL, Kishore, Kailas SV. Influence of roughness parameters and surface texture on friction during sliding of pure lead over 080 M40 steel. *The International Journal of Advanced Manufacturing Technology*. 2008;43:731.
- [38] Bowden FP, Bowden FP, Tabor D. *The friction and lubrication of solids*: Oxford university press; 2001.
- [39] Mikhlin N, Lyapin K. Hardness dependence of the coefficient of friction. *Russian Physics Journal*. 1970;13:317-21.
- [40] Rosenkranz A, Reinert L, Gachot C, Mücklich F. Alignment and wear debris effects between laser-patterned steel surfaces under dry sliding conditions. *Wear*. 2014;318:49-61.
- [41] Kalácska G. An engineering approach to dry friction behaviour of numerous engineering plastics with respect to the mechanical properties. *Express Polymer Letters*. 2013;7.
- [42] Kim E, Ko C, Kim K, Chen Y, Suh J, Ryu SG, et al. Site Selective Doping of Ultrathin Metal Dichalcogenides by Laser - Assisted Reaction. *Advanced Materials*. 2016;28:341-6.
- [43] Mao B, Siddaiah A, Zhang X, Li B, Menezes PL, Liao Y. The influence of surface pre-twinning on the friction and wear performance of an AZ31B Mg alloy. *Applied Surface Science*. 2019;480:998-1007.